CHAPTER 227

Numerical Simulations of Mud Transport by a Multi-Layered Nested Grid Model

Hiroichi Tsuruya[1]
Kazuo Murakami[1]
Isao Irie[2]

Abstract

A multi-layered model is developed for the prediction of mud transport in an estuary and ports to take into account the effects of submerged dikes and to reproduce the vertical distribution of suspended mud concentrations. A most remarkable result in the field observation in Kumamoto Port was the effect of a submerged dike on reducing the amount of deposition rate within the test trench.

It is predicted from the calculation that submerged dikes 1 m in height from the bottom will prevent siltation in the access channel and anchorages of Kumamoto Port by about 30% of the total deposition without submerged dikes.

1. Introduction

Extensive field measurements have been carried out in Kumamoto Port which is under construction to obtain detailed information on siltation mechanisms. Measured deposition rates within three trenches were used to calibrate the present model.

A nested grid model is adopted to treat the composite mesh arrangement of rough and fine meshes because the dimension of the trenches is so small, *i.e.*, 70m×50m in area.

The calculation is conducted with the supercomputer NEC SX-1E of the Port and Harbour Research Institute.

[1]Port and Harbour Research Institute, Ministry of Transport, 1-1, Nagase 3 Chome, Yokosuka, 239 Japan.
[2]Kyushu University, Dept. of Civil Engineering, 6-10-1, Hakozaki, Higashi-ku, Fukuoka, 812 Japan.

2. Mathematical Modeling of Mud Transport

For the treatment of the detailed configuration of the sea bed and construction such as submerged dikes, we adopted the multi-layered model with nested grid for the calculation of mud transport(Tsuruya et al., 1990). The present model consists of several horizontal layers as shown in Figure 1.

The water depth is vertically divided into seven layers as shown in Figure 2.

Tidal currents are calculated by a set of known equations: (1) continuity equations, and (2) equations of motion. Mud is transported in suspension and this process can be represented by diffusion equations.

Random wave deformations by refraction, wave breaking, diffraction, reflection are considered. Wave damping due to interaction between surface waves and a mud bed is also considered (Tsuruya et al., 1987b).

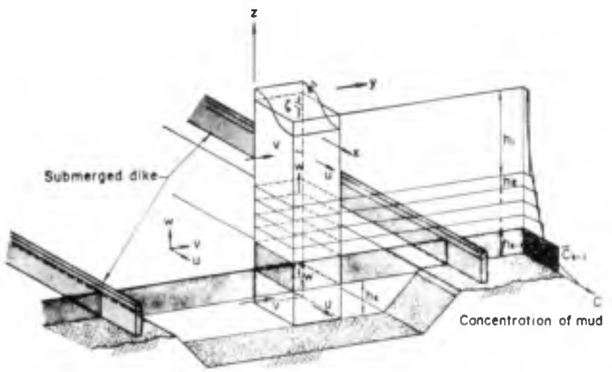

Figure 1. Multi-Layered Level Model

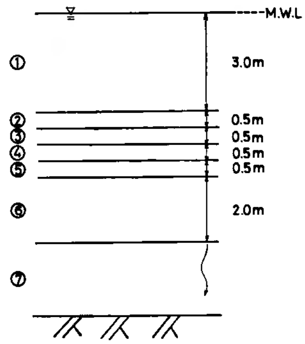

Figure 2. Division of Water Depth into Seven Layers

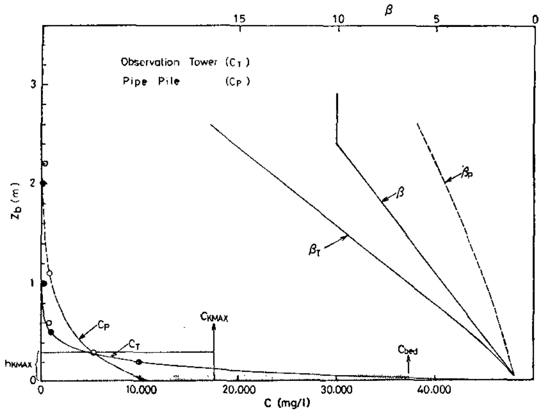

Figure 3. Vertical Distribution of SS and β

Erosion and Deposition

The rate of erosion of mud has been formulated by Partheniades (1965) as

$$E = M(\frac{\tau_b}{\tau_e} - 1), \tag{1}$$

where τ_b (Pa) is the shear stress at the bottom by the combined action of waves and currents, τ_e (Pa) the critical shear stress for erosion, and M ($kg/m^2/min$) is the constant. The bottom shear stress τ_b is given by Tanaka and Shuto (1981).

Deposition rate D is estimated by a similar consideration by Sheng and Lick (1979) as

$$\begin{aligned} D &= w_s C_{bed} \\ &= \beta w_s C_{KMAX}, \end{aligned} \tag{2}$$

where w_s is the settling velocity, C_{bed} the concentration of mud at the bed, and β is the correction factor to estimate C_{bed} from the calculated mean concentration of the bottom layer (C_{KMAX}). The correction factor β is introduced to estimate the concentration near the bottom from the calculated mean concentration C_{KMAX} at the bottom layer. The factor β may depend on the wave conditions, turbulence, the type of bed materials, and the thickness of the bottom layer. We now estimate the value of β from the field observation data. Figure 3 shows the typical distributions of SS observed at the observation tower and the pipe pile on August 31st, 1987. Plotted data are the average values of SS measured by water samplers.
Fitted curves are exponential functions and the concentration at the bed is assumed to be the average value

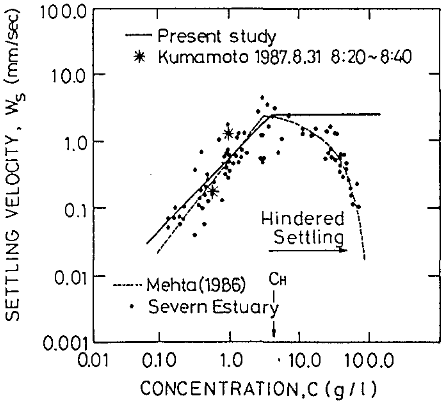

Figure 4. Relation between Settling Velocity and Concentration of Mud

from the bed to the height of 5 cm. Estimated value of β for each observation station are also shown in the figure as a function of the thickness of the bottom layer. We assume that the value of β is given by the average value obtained at the observation station and the pipe pile, and β is constant if the thickness of the bottom layer is larger than 2.4 m. The thick solid line in Figure 3 shows the functional relationship between the thickness of the bottom layer and β, given by the following expression as

$$\beta = \begin{cases} 1.0, (z_b \leqq 0.05\text{m}) \\ 3.9z_b + 0.805, (0.05 < z_b \leqq 2.4\text{m}) \\ 10.0, (z_b > 2.4\text{m}) \end{cases} \tag{3}$$

where z_b is the height from the bed and equal to the thickness of the bottom layer h_{KMAX}.

Settling Velocity

The settling velocity w_s for mud depends on the concentration. As the concentration increases, a probability of collision between mud particles increases and the settling velocity increases. Above some specific concentration, the settling velocity begins to decrease because of the hindered settling.

The relationship between the settling velocity w_s and mud concentration C is schematically shown in Figure 4. The broken line in the figure is given by Mehta (1986).

In the present model, hindered settling is not effectively applied because the erosion rate in this region will not be appropriately represented by Eq.(1). For the modeling of the process, more detailed research

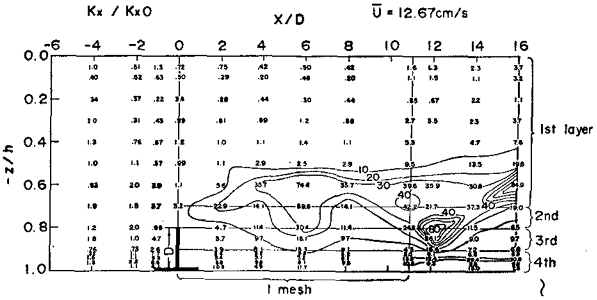

Figure 5. Rate of Increase in Horizontal Diffusion Coefficient

is required. Here we assumed that the settling velocity is constant for the concentration greater than the critical value C_H. Two asterisks in the figure are obtained by solving the diffusion equation in which the convection and diffusion terms are neglected.

Diffusion Coefficients behind Submerged Dikes

Turbulence intensity in the region behind a submerged dike increases considerably. Vertical and horizontal diffusion coefficients also increase when compared with cases without submerged dikes. The rate of increase in the diffusion coefficients with and without submerged dikes is investigated experimentally (Tsuruya et al., 1987a).

If the velocity is larger than the reference velocity U_{ref}, horizontal and vertical diffusion coefficients are increased according to the following expression as

$$\frac{K_H}{K_{H_0}} = [\frac{U_m}{U_{ref}}(K_H' - 1.0) + 1.0], \tag{4}$$

where K_H is the diffusion coefficient behind a submerged dike, K_{H0} the diffusion coefficient without a submerged dike, U_m the mean velocity in the second layer, U_{ref} the reference velocity (=25cm/s), and K_H' is the rate of increase in the diffusion coefficient which is given by the experiment. An example of the increase in the horizontal diffusion coefficient is represented in Figure 5.

3. Field Observations at Kumamoto Port

Kumamoto Port is under construction as a new commercial port at a site off-Kumamoto City in Ariake Bay.

Figure 6 shows the final plan of Kumamoto Port. The observation tower and the pipe pile which are shown by open circles were built at 4 m and 2 m depth, respec-

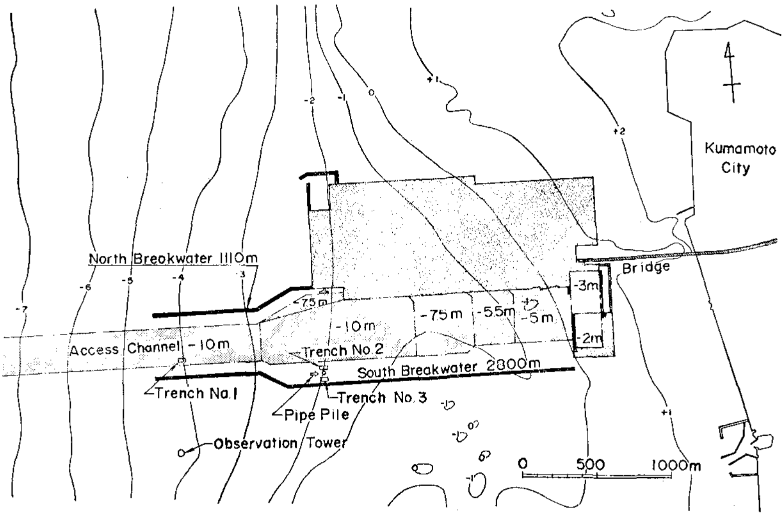

Figure 6. Plan of Kumamoto Port and Field Observation Site

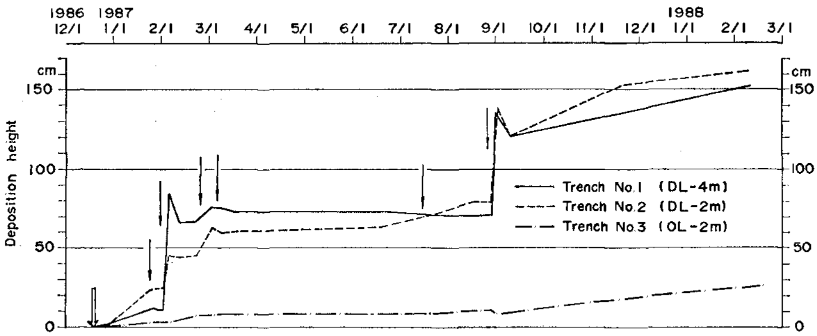

Figure 7. Time Variation of Deposition Heights at the Center of Three Trenches

tively, below the LWL to measure tides, waves, winds and turbidity of sea water.

Three trenches are constructed to investigate the relationship between the amount of sediment deposition and external forces such as waves and currents. The effect of a submerged dike to reduce the amount of deposition is also tested. Three trenches are shown in Figure 6. Trench No.1 is located at 4 m depth below LWL, and trenches No.2 and 3 are located at 2 m depth below LWL. Trench No.3 is surrounded by a submerged dike of 1m in height. On the other hand, trench No.2 is surrounded by no facility. The dimension of the trenches is 70m×50m in area. Trenches No.2 and No.3 are located 100 m apart from each other. The depth of the trenches is 2 m from the bed level and the side slope is 20 %.

Siltation Rate in Trenches

Figure 7 shows the time variation of deposition heights at the center of each trench. In the figure, six arrows show the onset of large waves. The leftmost arrow shows the start of the observation. It is found from the figure that the severe and sudden deposition occurred at

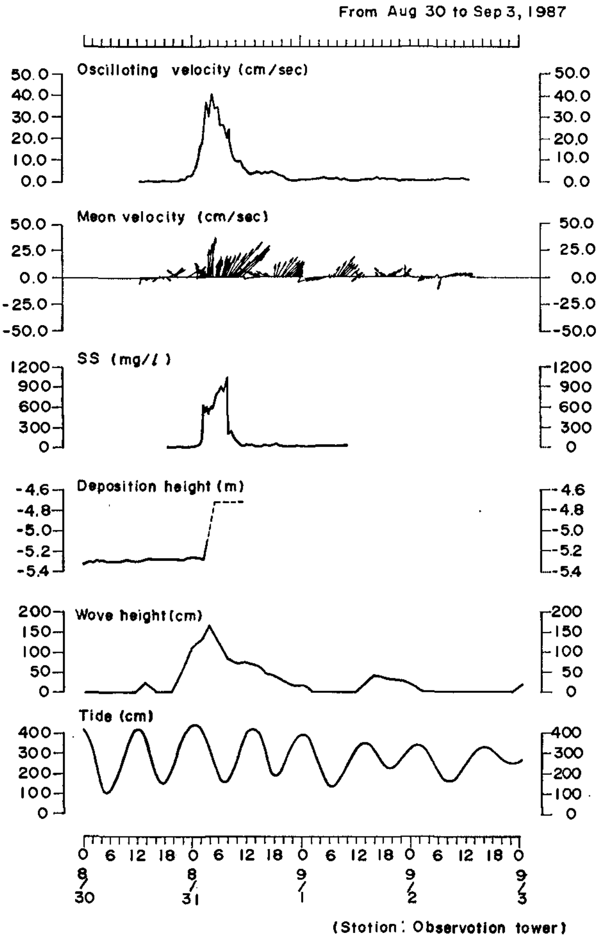

Figure 8. Example of Measured Time Series Data from Aug. 30 to Sept. 3, 1987 at Observation tower

trenches No.1 and No.2 during rough seas on February 3rd, 1987 and on August 31st, 1987. On the other hand, the deposition at trench No.3 was small. It is considered that the submerged dike has a considerable effect on reducing the deposition of mud. During gentle and calm seas, a small amount of deposition occurred in three trenches. This fact means that the tidal current has little effect on the deposition. Around the submerged dike, no extreme erosion and deposition could be observed.

The simultaneous measurements of tides, currents, turbidity, and bottom levels were carried out. Figure 8 shows the measured time series data of the oscillatory current velocity, averaged current vector, turbidity concentration, deposition height in trench No.1, wave height, and tidal level at the observation tower from August 30th to September 2nd, 1987. From the figure, it is found that there is a strong correlation between the oscillatory current velocity and the turbidity concentration. Moreover, increase of the bottom level starts when wave height is large and tidal level is low. It is suspected that the bottom sediments around Kumamoto Port are eroded mainly by wind waves. Also, the bottom sediments were eroded by stormy waves when the tidal level was low.

4. Calibration

Figure 7 shows the abrupt deposition occurred on February 6th and September 1st. We adopt the deposition on September 1st as the representative case for the

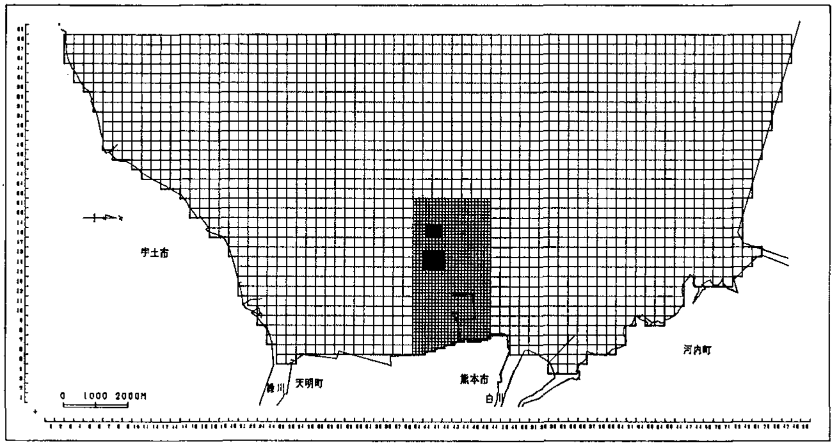

Figure 9. Mesh Map for the First Area

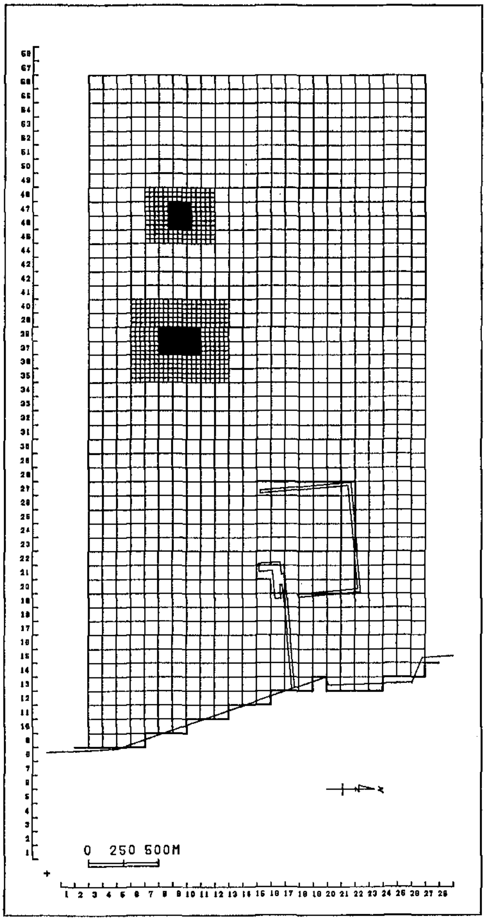

Figure 10. Mesh Map for the Second Area

calibration. Part of port facilities had been constructed at that time. The "Kumamoto Port Ohashi" bridge with a length of 872m, connecting the offshore port and the city, a wharf with a length of 300 m, and part of the revetment for a reclaimed land were completed.

The area for calculation is divided into five areas from the first to the fifth. Mesh sizes are 300m, 100m, and 100/3m for each area from the first to the third, respectively. For the fourth and the fifth area, the mesh size is 100/9m. Arrangement of the mesh for the first area is presented in Figure 9. Magnified meshes for the second area are shown in Figure 10. The third area is separated into two parts. Within them, there exist the fourth and the fifth area. They are shown in Figure 10 as the solid rectangles because the mesh size is so fine (11.1m). The fourth area (the lower solid rectangle) includes No.2 and No.3 trenches. The present nested grid model can treat the composite mesh arrangement of rough and fine meshes. Therefore, calculation, which included the small area with special interest, can be efficiently conducted.

The predicted wave damping ratio of the pipe pile to the observation tower by the multi-layered viscous fluid model (Tsuruya et al., 1987b) was 0.56. This value agreed closely with the observation when wave heights are large, i.e., from 2:00 to 6:00 a.m., August 31st. In the calculation, the depth of the mud layer and water content are set to at 10 cm and 200 %, respectively.

From Figure 8, wave conditions are decided to be as follows: $H_{1/3}$ = 1.25 m, $T_{1/3}$ = 4 s, direction of the wave is WSW and their duration is 6 hours. When waves are large, the tidal level is low. Therefore waves are operated from 15:00 to 21:00 in the calculation as shown in Figure 11. Only tidal current is calculated from 0:00 to 15:00. Calculations of erosion, diffusion, and settlement are conducted from 15:00 to 27:00. All the calculations are finished at time 27:00.

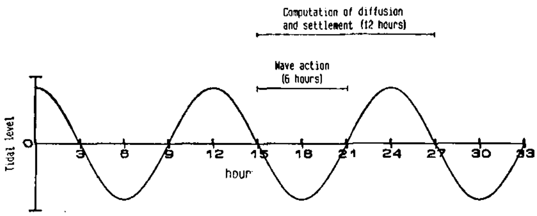

Figure 11. Time Table of Calculation

Tidal Currents

An example of the calculated tidal current distribution is shown in Figure 12. Velocities in the second area where the mesh is three times smaller than that of the first area are expressed together with the velocities for the first area.

Measured deposition heights during rough seas from August 31st to September 1st within three trenches are listed in Table 1 together with the water content.

In the calculation of erosion, the critical shear stress τ_e was set at 0.1 (Pa) after Murakami et al. (1989) and the constant M was varied until the reasonable deposition heights are obtained. The calculated deposition heights are listed in Table 2. The upper row

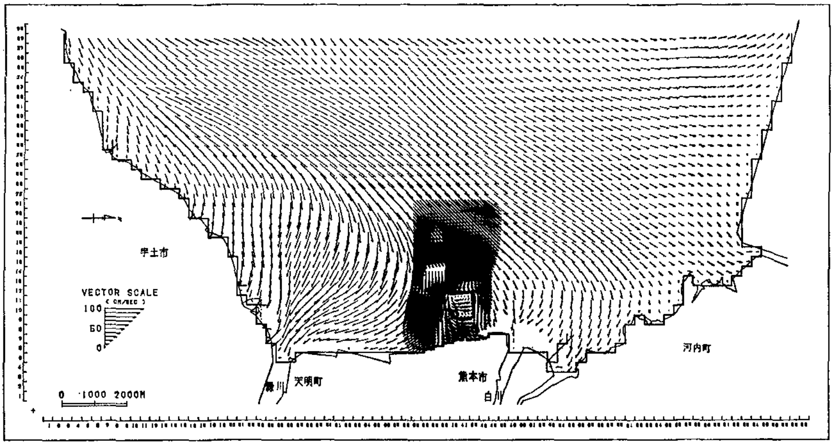

Figure 12. Calculated Velocity Distribution for the First Layer at the Maximum Flood Tide

Table 1. Deposition Heights and Water Contents within Three Trenches (Aug. 29 - Sept. 2, 1987)

	Trench No. 1	Trench No. 2	Trench No. 3
Deposition Height (cm)	63	60	−2
Water Content (%)	231	189	192

Table 2. Calculated Result of Deposition Heights

	Trench No. 1	Trench No. 2	Trench No. 3
Deposition (cm)	63.4	39.8	4.0
Deposition + Mass Transport (cm)	74.6	53.4	4.0

shows the contribution from deposition only and the lower one shows the total amount by both deposition and mass transport of the mud layer due to wave action. Comparing with Table 1, the calculated total deposition heights agree with the measured one. The value of M thus estimated 1.2 kg/m^2/min. According to van Leussen and

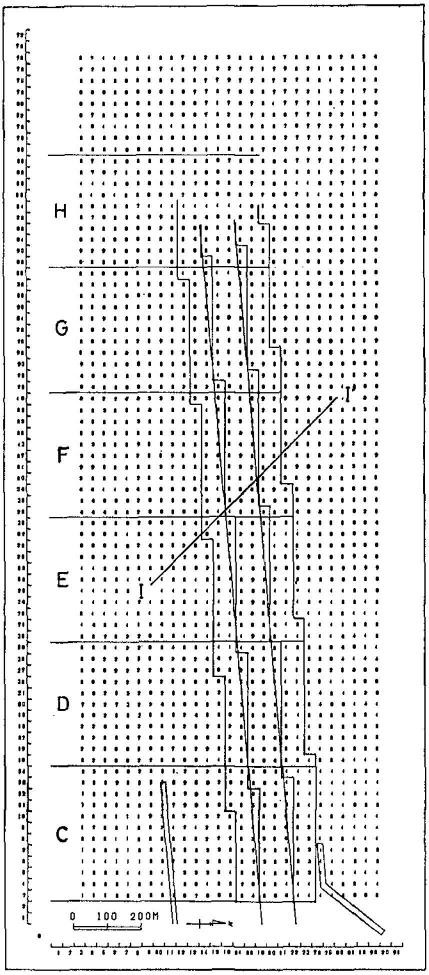

Figure 13. Access Channel

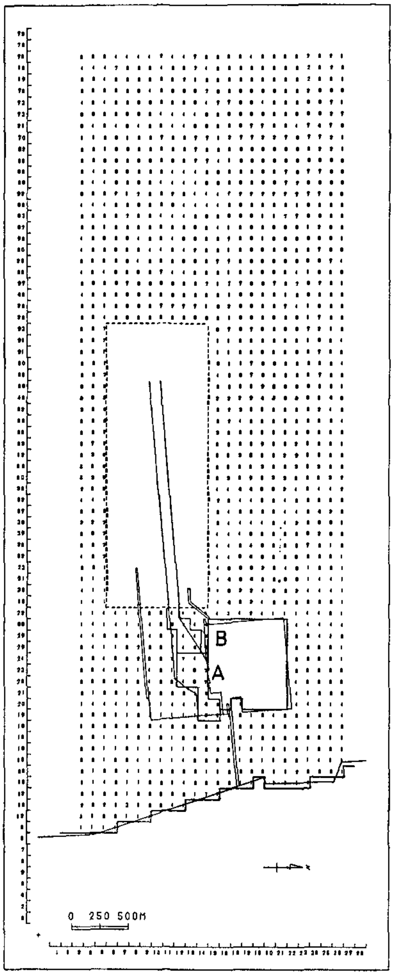

Figure 14. Anchorage

Dronkers (1988), the range of M is 0.006-0.24 $kg/m^2/min$. We have a larger value of M for the present model than usual. However, as the model does not include every process in the field, we must finally calibrate the calculated value with the field data. Therefore, we concluded that the present model could reproduce the deposition heights in the field.

5. Application to Future Plan of Kumamoto Port

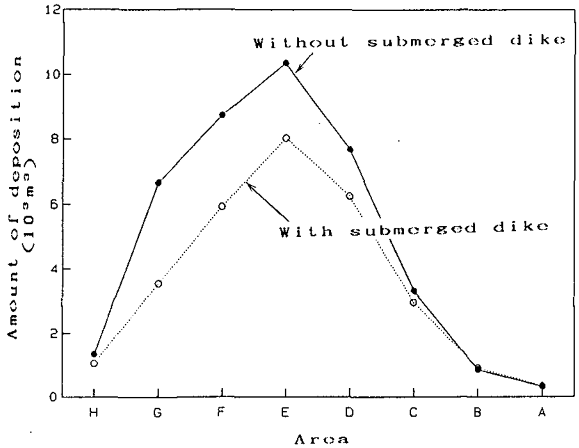

Figure 15. Amount of Deposition in Each Area

We show only the tentative plan that will be completed within a couple of years (Figures 13 and 14). In Figure 13, the access channel is 100m wide and 4.5m depth, and is shown as the inner parallel lines. The outer lines parallel to the access channel are submerged dikes which are 2,000m in length and 1m in height from the bottom. The calculated deposition heights inside the access channel are added together to get the volume of deposition for each area as shown in Figures 13 and 14. It is assumed that the water content of the deposited mud is 200%. The amount of deposition in each area is shown in Figure 15. The maximum deposition occurs at area E. The reducing effect of deposition by submerged dikes is about 23% for area E and 47% for area G. The calculated volume includes mass transport by waves. The amount of decrease in the volume of deposition owing to the submerged dike is about 30%.

6. Conclusions

Three-dimensional multi-layered level model with nested grid is developed for the calculation of siltation. After the calibration of deposition heights within three trenches, calculation for the future plan of Kumamoto Port is conducted. The amount of decrease in the volume of deposition due to submerged dikes was 30%.

Acknowledgements

We would like to express our appreciation to the Ministry of Transport and the Fourth District Port Construction Bureau for their support of the siltation research work project and for providing the field data.

We also thank Mr. Cao Zude, Chief Engineer of the Tianjin Research Institute of Water Transport Engineering, for analyzing the field data. Also, thanks are due to Mr. Hiroshi Yoshinaga, the member of Hydrodynamics Laboratory of the PHRI, for his assistance in typing the manuscript.

References

Mehta, A. J. (1986): Characterization of cohesive sediment properties and transport processes in estuaries, in Mehta A. J. (Ed), Estuarine Cohesive Sediment Dynamics, Lec. Notes Coastal Estuarine Stud. 14, pp.290-325.

Murakami, K., F. Suganuma and H. Sasaki (1989): Experimental investigation on erosion and deposition of fine cohesive sediments in an annular rotating channel, Report of the Port and Harbour Research Institute, Vol.28, No.1, pp.43-76 (in Japanese).

Partheniades, E. (1965): Erosion and deposition of cohesive soils, Proc. ASCE, Vol.91, No.HY1, pp.105-139.

Sheng, Y. P. and W. Lick (1979): The transport and resuspension of sediments in a shallow lake, J. Geopys. Res., Vol.84, No.C4, pp.1809-1826.

Tanaka, H. and N. Shuto (1981): Friction coefficient for a wave-current coexistent system, Coastal Engineering in Japan, Vol.24, pp.105-128.

Tsuruya, H., Y. Matsunobu, T. Korezumi and S. Yanagishima (1987a): Measurements of turbulent flow downstream of a submerged structure, Report of the Port and Harbour Research Institute, Vol.26, No.2, pp.127-169 (in Japanese).

Tsuruya, H., S. Nakano and J. Takahama (1987b): Interactions between surface waves and a multi-layered mud bed, Report of the Port and Harbour Research Institute, Vol.26, No.5, pp.137-173.

Tsuruya, H., K. Murakami and I. Irie (1990): Mathematical modeling of Mud Transport in Ports with a Multi-Layered Model -Application to Kumamoto Port-, Report of the Port and Harbour Research Institute, Vol.29, No.1, pp.3-51.

van Leussen, W. and J. Dronkers (1988): Physical Processes in estuaries: An introduction, in Dronkers, J. and W. van Leussen (eds), Physical processes in estuaries, Springer-Verlag, pp.1-18.